



**Non-equilibrium organosilane plasma polymerization for modulating the surface of PTFE towards potential blood contact applications**

Journal:	<i>Journal of Materials Chemistry B</i>
Manuscript ID	TB-ART-12-2019-002757.R1
Article Type:	Paper
Date Submitted by the Author:	31-Jan-2020
Complete List of Authors:	VIJAYAN, VINEETH; University of Alabama at Birmingham Tucker, Bernabe; University of Alabama at Birmingham Bobba , Pratheek ; University of Alabama at Birmingham Hwang, Patrick; Endomimetics LLC Catledge, Shane; University of Alabama at Birmingham, Physics Vohra, Yogesh; University of Alabama at Birmingham, Director, UAB Center for Nanoscale Materials Jun, Ho-Wook; U of Alabama at Birmingham, Biomedical Engineering Thomas, Vinoy; University of Alabama at Birmingham,

1       **Non-equilibrium organosilane plasma polymerization for modulating the**  
2       **surface of PTFE towards potential blood contact applications**

3       Vineeth M. Vijayan<sup>a,b</sup>, Bernabe S. Tucker<sup>b</sup>, Patrick T.J. Hwang<sup>d</sup>, Pratheek S. Bobba<sup>c</sup>, Ho-Wook  
4       Jun<sup>c</sup>, Shane A. Catledge<sup>a</sup>, Yogesh K. Vohra<sup>a</sup>, Vinoy Thomas<sup>a,b\*</sup>

5                   <sup>a</sup>Center for Nanoscale Materials and Biointegration,

6                   <sup>b</sup>Department of Material Science and Engineering,

7                   <sup>c</sup>Department of Biomedical Engineering,

8       The University of Alabama at Birmingham, Birmingham, AL 35294, United States

9                   <sup>d</sup>Endomimetics, LLC, Birmingham, Alabama, 35203, United States.

10                   \*Corresponding author ([vthomas@uab.edu](mailto:vthomas@uab.edu))

11  
12  
13       Abstract: We report a novel and facile organosilane plasma polymerization method designed to  
14       improve the surface characteristics of poly(tetrafluoroethylene) (PTFE). We hypothesized that  
15       the polymerized silane coating would provide an adhesive surface for endothelial cell  
16       proliferation due to high amount of surface hydroxyl groups, while the large polymer networks  
17       on the surface of PTFE would hinder platelet attachment. The plasma polymerized PTFE  
18       surfaces were then systematically characterized via different analytical techniques such as FTIR,  
19       XPS, XRD, Contact angle, and SEM. The key finding of these characterizations is the time-  
20       dependent deposition of an organosilane layer on the surface of PTFE. This layer was found to  
21       endow favorable surface properties to PTFE such as very high surface oxygen content, high  
22       hydrophilicity and improved surface mechanics. Additionally, *in vitro* cellular studies were  
23       conducted to determine the bio-interface properties of the plasma-treated and untreated PTFE.  
24       The important result of these experiments was rapid endothelial cell growth and decreased  
25       platelet attachment on the plasma-treated PTFE compared to untreated PTFE. Thus, this new  
26       surface modification technique could potentially address the current challenges associated with

27 PTFE for blood contact applications, specifically poor endothelial cell growth and risk of  
28 thrombosis.

## 29 **1. Introduction**

30 Surface modification is one of the widely used routes to augment biomaterials for appropriate  
31 cell responses. Plasma treatment/polymerization is a facile surface modification technique for  
32 polymers that has been employed for decades.<sup>1,2</sup> The nondestructive and in-situ sterilization  
33 capabilities of this technique makes it an attractive candidate for modifying the surface  
34 properties of biomaterials without compromising bulk properties. Plasma, the fourth state of  
35 matter, is composed of mixtures of ions, electrons, radicals, and neutral atoms/molecules which  
36 upon colliding on the surface of materials can rearrange or alter their surface chemistry.<sup>3,4</sup> It can  
37 introduce various surface functional groups such as amino, carboxyl and hydroxyl groups on the  
38 surface.<sup>5</sup> These functional groups can be further conjugated with various biomolecules, growth  
39 factors or peptides for a variety of biomedical applications.<sup>6,7</sup> Surface properties of biomaterials  
40 are very critical in determining the protein/cellular responses which in turn will decide the  
41 success rate of the implant biomaterials inside the body. Chemical surface modification is  
42 typically accomplished through performing certain surface reactions by wet chemistry.<sup>8</sup> This  
43 process is time consuming and can also lead some residual chemicals over the surface. This can  
44 affect the functional performance of the material inside the body. The absence of multiple  
45 reagents that wet chemistry uses for surface functionalization, thus, makes plasma as a safe,  
46 alternative method for surface modification of biomaterials.<sup>9</sup> Plasma surface modification is a  
47 simple and robust method, which can safely and reliably modify the surface properties of  
48 biomaterials towards different biomedical applications. However, the plasma surface  
49 modification of biomaterials is typically accomplished by using conventional feed gases such as

50 oxygen, ammonia, nitrogen and hydrogen.<sup>10-13</sup> These gases can introduce different functional  
51 groups such as carboxyl, amino and hydroxyl groups. However, these conventionally modified  
52 surfaces are always subject to ageing (surface reorganization); thus, ageing hinders the long-term  
53 ability to retain material properties associated with better cellular responses.<sup>14,15</sup>

54 Plasma has an interesting capability to induce polymerization of volatile organic  
55 monomers through a process called plasma enhanced chemical vapor deposition (PECVD); the  
56 polymers can be deposited over the surface of the substrate.<sup>16,17</sup> The high energy species formed  
57 as a result of this process causes a chain of reactions and, subsequently, causes the  
58 polymerization of the reactive monomer. But, unlike conventional polymers, plasma based  
59 polymers are not well organized they have a random arrangement.<sup>18</sup> Recently, plasma  
60 polymerization has played a major role in tissue regeneration applications.<sup>19</sup> Plasma  
61 polymerization of reactive monomers can tailor the surface properties of polymeric biomaterials  
62 to endow them with favorable cellular responses. More specific examples of such recent studies  
63 are plasma polymerization of organic monomers like acrylic acid and allyl amine on polymeric  
64 biomaterials.<sup>20-22</sup> Results of these studies suggest that these organic monomers when plasma  
65 polymerized, endow the polymer biomaterials with better cell adhesion and proliferation  
66 capabilities. More importantly the stability studies conducted on them, specifically on plasma  
67 polymerized acrylic acid coatings, have exhibited high stability; suggesting their potential utility  
68 for different biomedical applications.<sup>23</sup> Hence, plasma polymerizations of organic monomers  
69 have a wide scope to tailor the surface properties of biomaterials for different biointerface  
70 applications.

71 PTFE is a fluoropolymer which is widely used as a vascular graft material.<sup>24,25</sup> The  
72 chemically inert nature of PTFE makes it an ideal implantable material. Even though the large

73 diameter PTFE vascular grafts ( $\geq 6\text{mm}$ ) have been reported as successful <sup>25</sup>, PTFE still has  
74 serious issues with respect to the small diameter vascular grafts ( $\leq 4\text{mm}$ ).<sup>26</sup> Some of the  
75 important challenges associated with small diameter PTFE vascular grafts are thrombosis and  
76 lack of endothelial cell growth. The hydrophobic nature of the PTFE makes it very difficult for  
77 the endothelial cells to attach and grow to a confluent layer. Hence, it is essential to tailor the  
78 surface properties of PTFE to meet the requirements of small diameter vascular grafts. One of  
79 the most important methods of modifying the surface properties of PTFE is plasma modification.  
80 Different types of plasma processing are reported for modifying the surface properties of PTFE.  
81 Most of them are oxygen plasma, ammonia plasma and hydrogen plasma processing.<sup>27-29</sup> The  
82 major drawback of these plasma surface modification routes is ageing (significant reduction in  
83 functional groups with time).<sup>30</sup> Moreover, post-processing multistep conjugations with peptides  
84 and antithrombotic agents are further needed to favor endothelial cell growth. Recently, there are  
85 hybrid process (plasma modification and chemical modification) which are reported to tailor the  
86 surface properties of PTFE for blood contact applications. <sup>31,32</sup> These processes utilized the  
87 combination of oxygen plasma with dopamine surface functionalization for improving the  
88 endothelial cell affinity and anti-thrombogenicity. However, these types of hybrid processes  
89 requires multiple chemical reagents with several steps and they are time consuming. Hence, a  
90 more efficient and facile method of surface modification of PTFE would be highly appreciated  
91 for blood contact applications. Plasma polymerizations of organic monomers are never explored  
92 to tailor the surface properties of PTFE for blood contact applications. Inspired from this idea, in  
93 the current study we explored the plasma polymerization of an organosilane precursor, more  
94 specifically tetraethoxysilane (TEOS) to modify the surface properties of PTFE for blood  
95 contact applications. We hypothesized that the plasma polymerization of TEOS will augment

96 favorable surface properties for PTFE towards potential blood contact applications. To best of  
97 our knowledge there are no reports exploring the plasma polymerization capability of this  
98 organosilane monomer for tailoring/modifying the surface properties of PTFE for blood contact  
99 applications.

## 100 **2. Materials and Methods**

101 PTFE substrate used for the plasma modification (Laboratory grade PTFE sheets) was  
102 purchased from Oil sleek company, USA. Harrick Plasma chamber (PDC-001-HP) used for the  
103 plasma surface modification was purchased from Harrick Plasma, New York, USA. The reagents  
104 used for the experiments such as tetraethoxysilane and acetone were purchased from Sigma  
105 Aldrich.

### 106 **2.1 Plasma polymerization of tetraethoxysilane on PTFE**

107 The PTFE sheets were cut into 3 cm × 1.2 cm (0.2mm thickness) pieces for plasma  
108 treatment. Briefly, the samples were washed with acetone for 30 min. before the plasma  
109 treatment to remove adsorbed impurities (if any) from the surface. The PTFE samples were then  
110 placed inside a Harrick Plasma chamber (PDC-001-HP) and a radiofrequency (13.56 MHz, 45  
111 W) were used for plasma treatment. The plasma polymerization process of TEOS was  
112 accomplished by using a combination of TEOS-Air system inside the plasma chamber. Briefly, 1  
113 mL of TEOS was placed on a glass slide adjacent to the PTFE samples inside the chamber,  
114 followed by applying a constant Air flow rate of 50 SCCM inside the chamber. The reduced  
115 pressure (500 mTorr inside the chamber) facilitates the formation of TEOS vapors. Different  
116 plasma treatment times such as 10, 20 and 30 min were employed for optimizing the plasma

117 polymerization process. Herein they are referred to as PTFE-t10, PTFE-t20 and PTFE-t30 which  
118 correspond to 10 min, 20 min, and 30 min respectively.

## 119 **2.2 Characterizations**

120 Fourier-transform infrared spectroscopy (FTIR) and x-ray photoelectron spectroscopy  
121 (XPS) were employed to elucidate the surface chemistry. The Bruker alpha FTIR spectrometer  
122 with ATR mode was used to acquire IR-absorption spectrum (ranging from 4000 to 400 cm<sup>-1</sup>).  
123 XPS spectra of plasma treated samples were obtained using a Phi 5000 Versaprobe made by Phi  
124 Electronics, Inc. (Chanhassen, WI USA). The X-ray source of this instrument is a  
125 monochromatic, focused, Al K-alpha source (E = 1486.6 eV) at 25 W with a 100 micrometer  
126 spot size. The Mg anode ( $\lambda=1253.6$  eV) was used at 300 W and a barium oxide neutralizer  
127 eliminated charging. The survey scans (4 scans averaged per analysis) were obtained using pass  
128 energy of 187.5 eV with a step size of 0.5 eV. The high resolution scans (8 scans average per  
129 analysis) were obtained with pass energy of 23.5 eV and a step size of 0.1 eV.

130 To measure the contact angle, the samples (n=3) and were mounted onto a glass slide.  
131 Contact angles were measured using the sessile drop method as reported previously at the room  
132 temperature.<sup>33</sup> The water droplet size was 5  $\mu$ L. Image J software was used to accurately  
133 measure the contact angle of the water droplets on the surface.

134 The x-ray diffraction (XRD) experiments were performed on an Empyrean x-ray  
135 diffractometer (Malvern Panalytical, UK) equipped with a Cu LFF HR x-ray tube at 30 kV  
136 tension and 10 mA current. The spectrum was recorded for the range of  $2\theta$  from 10 to 100. The  
137 structure and morphology of the plasma treated and untreated control PTFE tapes were  
138 characterized scanning electron microscopy (SEM) after sputter-coated with Au-Pd and observed

139 using a FE-SEM (Quanta FEG 650 from FEI, Hillsboro, OR) and images were taken at different  
140 magnifications.

141 Hardness and Young's modulus were measured using an MTS NanoIndenter XP having a  
142 Berkovich diamond tip with nominal radius of 50 nm. Tip calibration was tested on the fused  
143 silica standard (accepted Young's modulus of 72 GPa) before and after testing all PTFE samples.  
144 All indents, including those on silica, were made to a maximum load of 1.5 mN. The measured  
145 Young's modulus and hardness values were determined at maximum load. Young's modulus of  
146 the silica before and after testing the PTFE surfaces was  $71.9 \pm 1.0$  GPa and  $72.0 \pm 3.0$  GPa,  
147 respectively. Therefore, moduli from the silica standard did not vary by more than 6%. 15  
148 indents were made on each sample for statistical analysis.

### 149 **2.3 Cell culture condition**

150 Human aortic endothelial cells (HAECs) were purchased from Lonza, Inc and cultured in  
151 Endothelial Growth Media (EGM-2 BulletKit; Lonza, Walkersville, MD). HAECs were grown  
152 to 70%–80% confluence at normal cell culture conditions (37°C, 95% humidity, 5% CO<sub>2</sub>) before  
153 being seeded onto PTFE sheets.

### 154 **2.4 MTS assay on PTFE sheets**

155 Samples were prepared by cutting PTFE sheets with varying durations of plasma treatment into  
156 circles with diameters of 6.4 mm and then sterilizing them with UV light for 3 hours. The sterile  
157 samples were then placed into a 96-well plate. 9,000 HAEC cells in 200  $\mu$ L of media were  
158 seeded onto each sheet and cultured in an incubator at 37 °C. After culture, an MTS [3-(4,5-  
159 dimethylthiazol-2-yl)-5-(3-carboxymethoxyphenyl)-2-(4-sulfophenyl)-2H-tetrazolium] assay  
160 (CellTiter 96 solution, Promega Co.) was performed to quantify HAEC proliferation on the



161 sheets at 1, 3, and 5 days. HAEC proliferation was assessed on 5 PTFE sheets for each duration  
162 of plasma treatment.

### 163 **2.5 Live/Dead assay on PTFE sheets**

164 Samples were prepared by cutting the PTFE sheets into circles with diameters of 9.5 mm and  
165 then UV sterilizing them for 3 hours. The samples were then placed into 48-well plates and  
166 25,000 HAEC cells in 400  $\mu$ L of media were seeded onto each sheet. The cells were cultured at  
167 37  $^{\circ}$ C for 3 days. After 3 days of culture, viable cells on the sheets were stained by conducting a  
168 Live/Dead Viability assay (Molecular Probes Inc., OR). Stained cells were imaged using a Nikon  
169 fluorescent microscope and image J software.

### 170 **2.6 Human platelet adhesion on PTFE sheets**

171 Samples were prepared similarly to those of the LIVE/DEAD assay and placed in 48-well plates.  
172 Platelets (Innovative Research, Inc.) were diluted with Tyrode's solution to a concentration of 6  
173  $\times 10^8$  platelets/mL. Platelets were then seeded onto the sheets and allowed to incubate for 30  
174 minutes. The sheets were then removed from the plate and washed with PBS to remove free  
175 floating platelets. After staining the sheets with calcein AM solution, platelets were visualized  
176 with a Nikon fluorescent microscope and ImageJ software.

### 177 **2.7 SEM Imaging for PTFE Sheets**

178 Samples were prepared similarly to those in the LIVE/DEAD assay and placed in 48-well plates.  
179 25,000 HAEC cells in 400  $\mu$ L of media were seeded onto each sheet and the cells were cultured  
180 at 37  $^{\circ}$ C for 3 days. After culture, the cells were fixed with paraformaldehyde. The fixed samples

181 were dehydrated with ethanol. The PTFE sheets were imaged using a Quanta™ 650 FEG (FEI  
182 Co.) with an accelerating voltage of 10 kV.

### 183 **2.8 Cytoskeletal staining**

184 Samples of material were prepared and cells were cultured as described for the live/dead  
185 analysis. Post culture samples were washed with PBS (1X, 5 min); fixed with paraformaldehyde  
186 (4%, 20 min); washed with additional PBS (1X, 5 min, with added Triton X-100 (0.1%).  
187 Staining was conducted with 200  $\mu$ L of staining solution (PBS 1X, BSA 1%, DAPI 0.1  $\mu$ g/mL,  
188 Phalloidin-Rhodamine conjugate (Abcam, 1X conc.) under dark conditions for 40 min. Then, the  
189 samples were rinsed with PBS (1X, 5 min) and the cover slips were added before imaging with a  
190 Nikon fluorescent microscope and ImageJ to process the data.

### 191 **2.9 Statistical Analysis**

192 The number of specimens tested for each group was 5 (n=5). The obtained data in the present  
193 study were tested for statistical significance using ANOVA method (Using the GraphPad Prism  
194 software) and  $p \leq 0.05$  was defined as significant.

## 195 **3. Results and Discussion**

196 Plasma polymerization is a phenomenon in which vapors of an organic monomer undergo a  
197 series of chemical reactions in the plasma phase such as hydrolysis and condensation and get  
198 polymerized. TEOS is one such monomer which can undergo plasma polymerization via the  
199 hydrolysis and condensation reactions. The silica polymerization is usually accomplished via a  
200 sol-gel reaction in wet chemistry methods. However, plasma based polymerization doesn't  
201 require the usage of any bases, solvents and high temperature. Hence, it is a far greener method

202 in comparison with the conventional sol-gel method. In the current work, we have employed the  
203 plasma polymerization capability of TEOS to polymerize and modify the surface properties of  
204 PTFE, which is a widely used vascular graft material. Air plasma was combined with the vapors  
205 of TEOS to facilitate the necessary hydrolysis and condensation reactions to form a plasma  
206 polymerized silane coating over the surface of PTFE (Scheme 1). To optimize our process of  
207 surface modification of PTFE with the silane derivative, we have comprehensively assessed the  
208 influence of the polymerization time over the surface of PTFE. More specifically, we have used  
209 different time intervals such as 10, 20 and 30 min of plasma polymerization of TEOS over PTFE.  
210 These 3 different plasma polymerized PTFE batches are referred to as PTFE-t10, PTFE-t20 and  
211 PTFE-t30 respectively. FTIR spectral comparison of pristine PTFE with PTFE-t10, PTFE-t20  
212 and PTFE-t30 has clearly shown additional bands specifically at  $3420\text{ cm}^{-1}$  (attributed to the OH  
213 stretching vibrations of the polymerized silane derivatives),  $1068\text{ cm}^{-1}$  (attributed to the Si-O  
214 stretching vibrations of the polymerized silane derivatives) (Fig 1a). More specifically, PTFE-t10  
215 and PTFE-t20 was exhibiting a clear peak emergence at the region of Si-O stretching vibrations.  
216 This suggested the plasma polymerization of silane over the surface of PTFE. The pristine PTFE  
217 only exhibited the characteristic stretching vibrations of  $-\text{CF}_2$  at  $1153\text{ cm}^{-1}$  and  $1210\text{ cm}^{-1}$  and  
218 rolling vibrations of  $-\text{CF}_2$  groups at  $635\text{ cm}^{-1}$ . This clearly supported our hypothesis that the  
219 possible plasma polymerization of the TEOS occurred over the surface of PTFE. In order to  
220 validate this point, as a control experiment we have also performed the surface modification of  
221 PTFE using air (ambient atmosphere as feed gas) plasma alone at similar time points. We found  
222 that the FTIR spectrum was exhibiting similar bands for both pristine and air plasma modified  
223 PTFE (Fig 1b). This clearly indicates that air plasma alone cannot impart any significant  
224 functionalization on PTFE surface. Also, it was clear that when TEOS vapors were combined

225 with air plasma it has clearly resulted in the plasma assisted polymerization of TEOS and  
226 subsequent deposition/modification of PTFE surfaces. Hence, taken together the FTIR spectral  
227 data was clearly suggesting the possible plasma polymerization and further modification of the  
228 silane derivative on PTFE. Further, we have employed another complementary technique to  
229 FTIR specifically, Raman spectral analysis, of the PTFE-t10, PTFE-t20 and PTFE-t30. Raman  
230 spectra have shown similar bands for both pristine PTFE and PTFE-t10, PTFE-t20 and PTFE-t30  
231 surfaces, interestingly, it was found that there was a clear peak emergence at  $854\text{ cm}^{-1}$  for the  
232 PTFE-t10, PTFE-t20 and PTFE-t30 in comparison with the pristine PTFE. This peak at  $854\text{ cm}^{-1}$   
233 can be assigned to hydrogen associated with silicon fluoride (H-Si-F) modes.<sup>34</sup> During the  
234 process of plasma polymerization of silane, the surface of the fluorinated polymer PTFE can get  
235 attached with the silicon and hydrogen atoms of the silane precursor (TEOS) to form H-Si-F type  
236 linkages on the surface. This process is expected to be time dependent; hence the corresponding  
237 peak also emerged more predominantly with respect to plasma polymerization time. (Fig1c).  
238 New additional peaks were also present at  $2899$ ,  $2932$  and  $2980\text{ cm}^{-1}$  (attributed to the  $-\text{CH}$   
239 stretching vibrations) for the PTFE-t20 in comparison with pristine PTFE (Fig 1d). It was worthy  
240 to note that PTFE-t10 and PTFE-t20 were showing the most predominantly emerged additional  
241 peaks at this region. Hence, together both the FTIR and Raman spectra suggested the successful  
242 silane plasma polymerization process on PTFE. Further, we studied the surface chemistry  
243 changes taking place during the plasma polymerization process using the XPS. The XPS spectra  
244 of the PTFE-t10, PTFE-t20 and PTFE-t30 surfaces have clearly shown the presence of silica and  
245 surface oxygen (Fig 2a). The oxygen and silica atomic percentages over the surface have  
246 depicted a time dependent behavior with respect to the plasma polymerization time. More  
247 specifically, the amount of both oxygen and silica increased when the polymerization time was

248 increased from 10 to 20 min and afterwards it started decreasing at 30 minutes (Table S1). This  
249 can be attributed to the fact that the plasma polymerization process of TEOS at short time scale  
250 progresses well, and after reaching a point it get saturated, then reaches equilibrium. This is  
251 followed by the phenomenon of surface etching that can reduce the polymerization products  
252 through ablation. The control experimental set (air plasma modified PTFE surfaces) has not  
253 shown any significant changes in the elemental composition or the presence of silica or higher  
254 oxygen content with respect to the pristine PTFE (Fig 2b). The high resolution C1s spectrum of  
255 pristine PTFE has shown two important peaks at 291 eV (attributed to the C-F bonds) and 284  
256 eV (attributed to the C-C bonds present in the surface) (Fig 2c). Interestingly, the PTFE-t10,  
257 PTFE-t20 and PTFE-t30 were clearly exhibiting an increased percentage of the C-C bonds with  
258 respect to time. More specifically, it was seen that PTFE-t10 and PTFE-t20 were showing  
259 increase in C-C bond percentage while for PTFE-t30 it was found to decrease. Thus, XPS spectra  
260 were also supporting the successful silane plasma polymerization process over PTFE. Further,  
261 we have studied the XPS surface chemical mapping on PTFE, PTFE-t10, PTFE-t20 and PTFE-  
262 t30 . The chemical mapping of pristine PTFE has shown the presence of carbon and Fluorine  
263 only on the surface. The surface mapping of PTFE-t10, PTFE-t20 and PTFE-t30 has clearly  
264 shown the additional presence of oxygen (from TEOS) and silica (from TEOS) (Fig 3). Hence,  
265 the surface chemical mapping has strongly suggested the plasma polymerization and subsequent  
266 deposition of a silane layer on PTFE surface. Further, we have systematically evaluated the water  
267 contact angle on PTFE, PTFE-t10, PTFE-t20 and PTFE-t30. There was a drastic reduction in the  
268 water contact angle of the PTFE-t10, PTFE-t20 and PTFE-t30 surfaces in comparison with the  
269 pristine PTFE (Fig 4a). More specifically, with water contact angle of  $102^{\circ} \pm 1.23$  (for pristine  
270 PTFE),  $25^{\circ} \pm 1.54$  (for PTFE-t10),  $61^{\circ} \pm 1.76$  (for PTFE-t20) and  $64^{\circ} \pm 2.01$  (for PTFE-t30). The

271 wettability measurements suggested that PTFE-t10 produced the most hydrophilic surface  
272 modification. The observed high hydrophilicity of the PTFE-t10 may be attributed to the  
273 presence of multiple numbers of surface hydroxyl groups that are generated through the plasma  
274 polymerization process. However, after reaching saturation, the surface etching phenomenon  
275 predominates the surface coating process, this may be increase the surface roughness and thereby  
276 increasing the hydrophobic behavior at longer plasma exposure times. XRD analysis was  
277 performed to study the effect of plasma polymerization on the crystalline behavior of PTFE. It  
278 was found that both pristine PTFE and PTFE-t10, PTFE-t20 and PTFE-t30 exhibited highly  
279 crystalline behavior with narrow peak at  $2\theta$   $18.018^\circ$  (100 plane) (Fig 4b). However, up on close  
280 looking this characteristics peak, it was found that the peak position slowly increased for the  
281 PTFE-t10 and PTFE-t20 ( $18.084^\circ$  &  $18.17^\circ$ ) (Fig 4c). The PTFE-t30 has shown a slight decrease  
282 in the peak position to that of pristine PTFE,  $17.87^\circ$ . This observed trend can be attributed to the  
283 fact that the plasma polymerization/deposition can induce strain in the crystal lattice during the  
284 silane coating process. This may be the reason for the observed peak shift from the pristine  
285 PTFE. However, for the PTFE-t30 .the surface etching become more predominant and the strain  
286 in the lattice offered by the polymerized layer may have got decreased rapidly, this may be the  
287 reason for the observed peak shift towards lower values. We hypothesized that the plasma  
288 polymerization of the silane precursor and subsequent coating will reduce the surface roughness  
289 of PTFE and will make the surface more smooth making it favorable for endothelial cell  
290 adhesion and proliferation. In order to validate this hypothesis, we have employed the scanning  
291 electron microscopy evaluation of the surface features on PTFE, PTFE-t10, PTFE-t20 and  
292 PTFE-t30. It was found that the pristine PTFE were having irregular surface topography with  
293 high irregularities and roughness. The PTFE-t10, and PTFE-t20 surfaces were clearly exhibiting

294 smoother surface topography with much less surface irregularities and roughness (Fig 5a).  
295 During longer plasma exposure time, along with the deposition of the polymerized layer, the  
296 process of surface etching from the plasma becomes predominant. This was clearly visualized for  
297 PTFE-t30 where the surface etching of the plasma polymerized layer and the etched coating can  
298 be clearly visualized on the surface. This observation was consistent with respect to XPS results,  
299 which was showing that this process of plasma polymerization after reaching a threshold for  
300 PTFE-t20 got reduced significantly and destabilizes or surface etching happens for PTFE-t20,  
301 suggesting the possible surface etching phenomenon. The plasma polymerized surface coating  
302 was clearly visualized by comparing two different regions in PTFE (one with coating and the  
303 other one without any plasma coating). It was seen that the region which was exposed for plasma  
304 polymerization was clearly exhibited surface coating in compared to the region unexposed to  
305 plasma polymerization (Fig S2). The inferences drawn from the SEM imaging was further  
306 supported by the 3D laser scanning confocal microscope (Fig 5b). It was seen that for PTFE-t30,  
307 the surface was clearly having significant height differences which indicates potential surface  
308 etching taking place. Taken together, the SEM and laser scanning microscopy were showing that  
309 plasma polymerization has resulted in the deposition of a silane polymerized layer over PTFE. It  
310 was also found that this modification is more stable for PTFE-t10 and PTFE-t20 in comparison  
311 with PTFE-t30. The surface mechanical properties of PTFE are relevant to consider for various  
312 biomedical applications. Hence, we have compared the surface mechanics on PTFE-t10, PTFE-  
313 t20 and PTFE-t30 at different time points through nanoindentation studies (Fig 6a). The surface  
314 modulus and hardness exhibited by the pristine PTFE sheet was consistent with respect to the  
315 previously reported values for PTFE.<sup>35</sup> Furthermore, the nanoindentation studies indicate that the  
316 PTFE-t20 and PTFE-t30, have increased Young's modulus and hardness in comparison with

317 pristine PTFE and PTFE-T10. The load/displacement curves (Fig 6a) confirm the plastic depth of  
318 indentation to decrease significantly from as high as 57% for the pristine PTFE and PTFE-T10  
319 samples to as low as 34% for the PTFE-T30 sample. The modulus and hardness results are  
320 summarized in Fig 6b and 6c and in Table S3. Hence, it was clear that this plasma polymerized  
321 silane coating not only contributed in making hydrophilic PTFE surface but also improved the  
322 surface mechanical properties of the PTFE, depending on the polymerization time. It is  
323 noteworthy that PTFE and PTFE-T10 have exhibited no significant change in elastic modulus or  
324 hardness due to thin-layer surface polymerization. This could be beneficial for their use towards  
325 cardiovascular applications where there is need for flexibility of a vascular graft with systolic  
326 and diastolic pressures.

327         Thrombosis and poor endothelial cell attachment are one of the major drawbacks for  
328 PTFE towards blood contact applications. We hypothesized that our modified surfaces with both  
329 high surface oxygen content and high hydrophilicity could address these existing challenges. In  
330 order to validate this hypothesis, we studied endothelial cell behaviors on PTFE, PTFE-t10,  
331 PTFE-t20. First, we conducted live/dead cell assay and the PTFE-t10 and PTFE-t20 exhibited  
332 higher number of live endothelial cells than the pristine PTFE at 3 days (Fig 7a). Next, to obtain  
333 quantitative information on the proliferation of the endothelial cells on the plasma polymerized  
334 PTFE surfaces, we performed the MTS assay for different time points such as 1,3 and 5 days  
335 (Fig 7b). The PTFE-t10 and PTFE-t20 showed significantly higher endothelial cell proliferation  
336 than the pristine PTFE group at 3 and 5 days. Platelet adhesion studies were further done to  
337 assess the thrombogenicity of the plasma polymerized PTFE surfaces. Interestingly, the PTFE-  
338 t10 and PTFE-t20 have shown significantly less adhesion of platelets compared to pristine PTFE  
339 surfaces (Fig7c). Thus the platelet adhesion studies were suggesting the potential non



340 thrombogenicity of the PTFE-t10 and PTFE-t20 surface. Albumin is the most abundant protein  
341 in the blood plasma which when adsorbed on the surface of vascular prosthesis found to reduce  
342 the nonspecific protein adsorption cascades and reduce the thrombosis.<sup>36</sup> Hence, we have  
343 performed a preliminary qualitative albumin adsorption study on PTFE-t10. More specifically  
344 FITC tagged bovine serum albumin (BSA) protein adsorption studies were done to compare the  
345 albumin adsorption between pristine PTFE and PTFE-t10. Very bright fluorescence was  
346 observed from PTFE-t10 in comparison with pristine PTFE surfaces (Fig S4a). This was clearly  
347 suggesting the higher albumin adsorption on PTFE-t10. This may be the reason for the observed  
348 low platelet adhesion of the PTFE-t10 in comparison with the pristine PTFE surfaces. The  
349 observed higher BSA adsorption also supported the higher endothelial cell proliferation on  
350 PTFE-t10. Polymers like polyethylene glycol (PEG) were found to exhibit similar antifouling  
351 properties due to a number of factors such as steric effect, hydration and chain mobility.<sup>37</sup> We  
352 hypothesize that the observed trend of low platelet adhesion on PTFE-t10 and PTFE-t20 surfaces  
353 can be also attributed to the similar effects which can be offered by the random silane polymer  
354 chains such as steric effect, hydration (due to very high number of surface hydroxyl groups) and  
355 random polymer chains (which is hallmark of plasma polymerization process).

356 SEM imaging of the fixed endothelial cells on PTFE-t10, PTFE-t20 and pristine PTFE  
357 surface also showed a drastic difference in their morphology. Interestingly, the 10 min plasma  
358 polymerized PTFE surface has clearly showed more spreaded endothelial cells with formation of  
359 pseudopods when compared to the pristine PTFE (Fig S4b). We also observed a similar trend of  
360 cell adhesion through the phalloidin cytoskeleton staining. The plasma polymerized PTFE  
361 surfaces exhibited cell sprouting and the images showed extended cytoskeleton when compared  
362 to the pristine PTFE (Fig 8). The observed higher endothelial proliferation and cytoskeleton

363 spreading on PTFE-t10, PTFE-t20 can be attributed to a number of factors such as very high  
364 surface oxygen content, high hydrophilicity and a smooth surface (offered by the coating). Taken  
365 together, the endothelial cell proliferation and platelet adhesion studies suggested that the PTFE-  
366 t10, PTFE-t20 surfaces were found to exhibit good endothelial cell adhesion with low platelet  
367 adhesion. The observed phenomenon of low platelet adhesion and higher endothelial cell  
368 proliferation was consistent with the previously reported chondroitin sulfate coating on PET  
369 surfaces for vascular implants.<sup>38</sup> This study attributed the higher endothelial cell adhesion to the  
370 presence of negatively charged surface chondroitin sulfate coating which can selectively adsorb  
371 fetal bovine serum (FBS) proteins or growth factors. We hypothesize that in our present plasma  
372 polymerized silane coating having very high number of surface hydroxyl groups can bind  
373 selectively to FBS proteins similar to that of the chondroitin sulfate coating that can facilitate  
374 more endothelialization.

#### 375 **4. Conclusions**

376 In conclusion, we report a new facile organosilane plasma polymerization method to tailor the  
377 surface properties of PTFE. We hypothesized that the plasma polymerization of silane can  
378 augment the PTFE surface properties with characteristics such as high hydrophilicity, high  
379 surface oxygen content and improved endothelial cell adhesion. This hypothesis was clearly  
380 justified by the material and biological characterization performed on the plasma modified PTFE  
381 surfaces. The results of different techniques such as FTIR, XPS, XRD and SEM have clearly  
382 proved the successful plasma polymerization and subsequent coating of hydrophilic thin layer on  
383 the surface of PTFE. The endothelial cell proliferation and platelet adhesion studies have shown  
384 that the plasma polymerized PTFE surfaces favored good endothelial cell adhesion with minimal  
385 platelet adhesion. More importantly, the reported method was a facile single step surface

386 modification technique which doesn't require any further post modification steps to augment  
387 PTFE surfaces with better endothelial cell adhesion and reduced platelet adhesion. Taken  
388 together, these results suggest the potential of this methodology towards potential blood contact  
389 applications.

## 390 **5. Acknowledgments**

391 This work was supported by funding through NSF EPSCoR RII-Track-1 Cooperative Agreement  
392 OIA-1655280. We also acknowledge the NSF Major Research Instrumentation (MRI) Grant No.  
393 DMR-1725016 for XRD facility. HWJ and PTH acknowledge the partial support from NIH  
394 1R01HL125391-01 and NIH 2R44DK109789-02. BT acknowledges the fellowship from  
395 Department of Education GAANN Grant No. P200A180001. Any statement, opinion,  
396 recommendation, or conclusions shared are those only of the authors and do not necessary relay  
397 the official positions of the National Science Foundation or the US Department of Education.  
398 V.M.V. expresses special thanks to Dr Paul Baker for assistance in XPS and XRD analysis.

## 399 **6. References**

- 400 1 C. Oehr, *Nucl. Instrum. Methods Phys. Res. Sect. B Beam Interact. Mater. At.*, 2003, **208**, 40–  
401 47.
- 402 2 D. L. Elbert and J. A. Hubbell, *Annu. Rev. Mater. Sci.*, 1996, **26**, 365–394.
- 403 3 P. Chu, *Mater. Sci. Eng. R Rep.*, 2002, **36**, 143–206.
- 404 4 R. N. S. Sodhi, *J. Electron Spectrosc. Relat. Phenom.*, 1996, **81**, 269–284.
- 405 5 R. Landgraf, M.-K. Kaiser, J. Posseckardt, B. Adolphi and W.-J. Fischer, *Procedia Chem.*,  
406 2009, **1**, 1015–1018.

- 407 6 B. R. Coad, T. Scholz, K. Vasilev, J. D. Hayball, R. D. Short and H. J. Griesser, *ACS Appl.*  
408 *Mater. Interfaces*, 2012, **4**, 2455–2463.
- 409 7 K. S. Siow, L. Britcher, S. Kumar and H. J. Griesser, *Plasma Process. Polym.*, 2006, **3**, 392–  
410 418.
- 411 8 H. S. Sundaram, X. Han, A. K. Nowinski, N. D. Brault, Y. Li, J.-R. Ella-Menye, K. A.  
412 Amoaka, K. E. Cook, P. Marek, K. Senecal and S. Jiang, *Adv. Mater. Interfaces*, 2014, **1**,  
413 1400071.
- 414 9 A. A. John, A. P. Subramanian, M. V. Vellayappan, A. Balaji, S. K. Jaganathan, H. Mohandas,  
415 T. Paramalingam, E. Supriyanto and M. Yusof, *RSC Adv.*, 2015, **5**, 39232–39244.
- 416 10 A. Vesel and M. Mozetic, *Vacuum*, 2012, **86**, 634–637.
- 417 11 P. Chevallier, M. Castonguay, S. Turgeon, N. Dubrulle, D. Mantovani, P. H. McBreen, J.-C.  
418 Wittmann and G. Laroche, *J. Phys. Chem. B*, 2001, **105**, 12490–12497.
- 419 12 S. B. Idage and S. Badrinarayanan, *Langmuir*, 1998, **14**, 2780–2785.
- 420 13 N. Inagaki, S. Tasaka, K. Narushima and K. Teranishi, *J. Appl. Polym. Sci.*, 2002, **83**, 340–  
421 348.
- 422 14 J. Nakamatsu, L. F. Delgado-Aparicio, R. Da Silva and F. Soberon, *J. Adhes. Sci. Technol.*,  
423 1999, **13**, 753–761.
- 424 15 M. Modic, I. Junkar, A. Vesel and M. Mozetic, *Surf. Coat. Technol.*, 2012, **213**, 98–104.
- 425 16 M. C. Vasudev, K. D. Anderson, T. J. Bunning, V. V. Tsukruk and R. R. Naik, *ACS Appl.*  
426 *Mater. Interfaces*, 2013, **5**, 3983–3994.
- 427 17 F. Khelifa, S. Ershov, Y. Habibi, R. Snyders and P. Dubois, *Chem. Rev.*, 2016, **116**, 3975–  
428 4005.

- 429 18 A. Michelmore, J. D. Whittle, R. D. Short, R. W. Boswell and C. Charles, *Plasma Process.*  
430 *Polym.*, 2014, **11**, 833–841.
- 431 19 G. Aziz, R. Ghobeira, R. Morent and N. D. Geyter, in *Recent Research in Polymerization*, ed.  
432 N. Cankaya, InTech, 2018.
- 433 20 P. Cools, C. Mota, I. Lorenzo-Moldero, R. Ghobeira, N. De Geyter, L. Moroni and R.  
434 Morent, *Sci. Rep.*, , DOI:10.1038/s41598-018-22301-0.
- 435 21 R. Bitar, P. Cools, N. De Geyter and R. Morent, *Appl. Surf. Sci.*, 2018, **448**, 168–185.
- 436 22 X. Liu, Q. Feng, A. Bachhuka and K. Vasilev, *ACS Appl. Mater. Interfaces*, 2014, **6**, 9733–  
437 9741.
- 438 23 P. Cools, H. Declercq, N. De Geyter and R. Morent, *Appl. Surf. Sci.*, 2018, **432**, 214–223.
- 439 24 S. Roll, J. Müller-Nordhorn, T. Keil, H. Scholz, D. Eidt, W. Greiner and S. N. Willich, *BMC*  
440 *Surg.*, , DOI:10.1186/1471-2482-8-22.
- 441 25 E. A. Santiago-Delpin and T. Aviles, *Am. J. Surg.*, 1980, **140**, 315–319.
- 442 26 A. G. Nordestgaard, J. A. Buckels and S. E. Wilson, *Br. J. Exp. Pathol.*, 1986, **67**, 839–849.
- 443 27 S. Zanini, R. Barni, R. D. Pergola and C. Riccardi, *J. Phys. Appl. Phys.*, 2014, **47**, 325202.
- 444 28 S. D. Pringle, V. S. Joss and C. Jones, *Surf. Interface Anal.*, 1996, **24**, 821–829.
- 445 29. N. Inagaki, S. Tasaka and T. Umehara, *J. Appl. Polym. Sci.*, 1999, **71**, 2191–2200.
- 446 30. J. Nakamatsu, L. F. Delgado-Aparicio, R. Da Silva and F. Soberon, *J. Adhes. Sci. Technol.*,  
447 1999, **13**, 753–761.
- 448 31. H.-Y. Mi, X. Jing, J. A. Thomsom and L.-S. Turng, *J. Mater. Chem. B*, 2018, **6**, 3475–3485.
- 449 32. B. Cheng, Y. Inoue and K. Ishihara, *Colloids Surf. B Biointerfaces*, 2019, **173**, 77–84.
- 450 33. B. S. Tucker, P. A. Baker, K. G. Xu, Y. K. Vohra and V. Thomas, *J. Vac. Sci. Technol. A*,  
451 2018, **36**, 04F404.

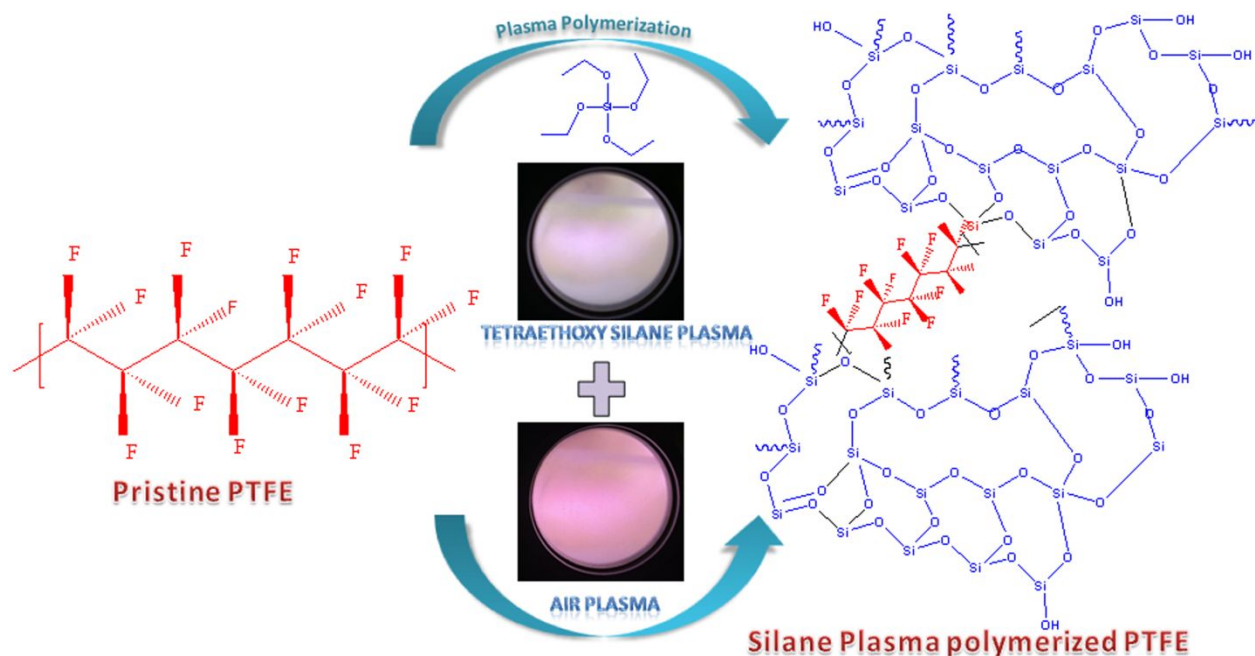
- 452 34. P. G. Spizzirri, J.-H. Fang, S. Rubanov, E. Gauja and S. Prawer, 2010 (arXiv:1002.2692).
- 453 35. I. C. Halalay, M. J. Lukitsch, M. P. Balogh and C. A. Wong, *J. Power Sources*, 2013, **238**,  
454 469–477.
- 455 36. B. Sivaraman and R. A. Latour, *Biomaterials*, 2010, **31**, 1036–1044.
- 456 37. L.-C. Xu and C. A. Siedlecki, *J. Biomed. Mater. Res. B Appl. Biomater.*, 2017, **105**, 668–678.
- 457 38. K. Thalla, H. Fadlallah, B. Liberelle, P. Lequoy, G. De Crescenzo, Y. Merhi and S. Lerouge,  
458 *Biomacromolecules*, 2014, **15**, 2512–2520.

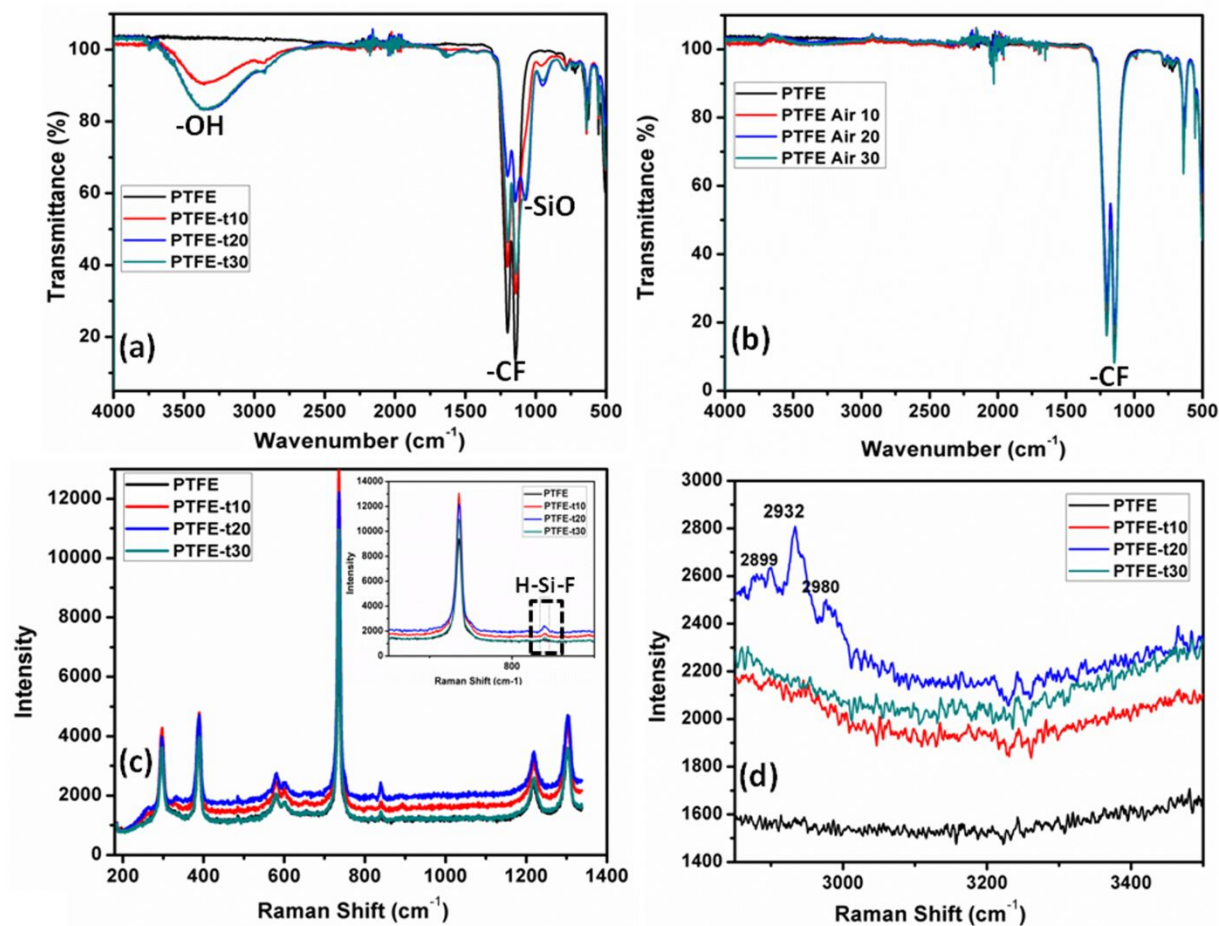
459

460

### Figures

461





465

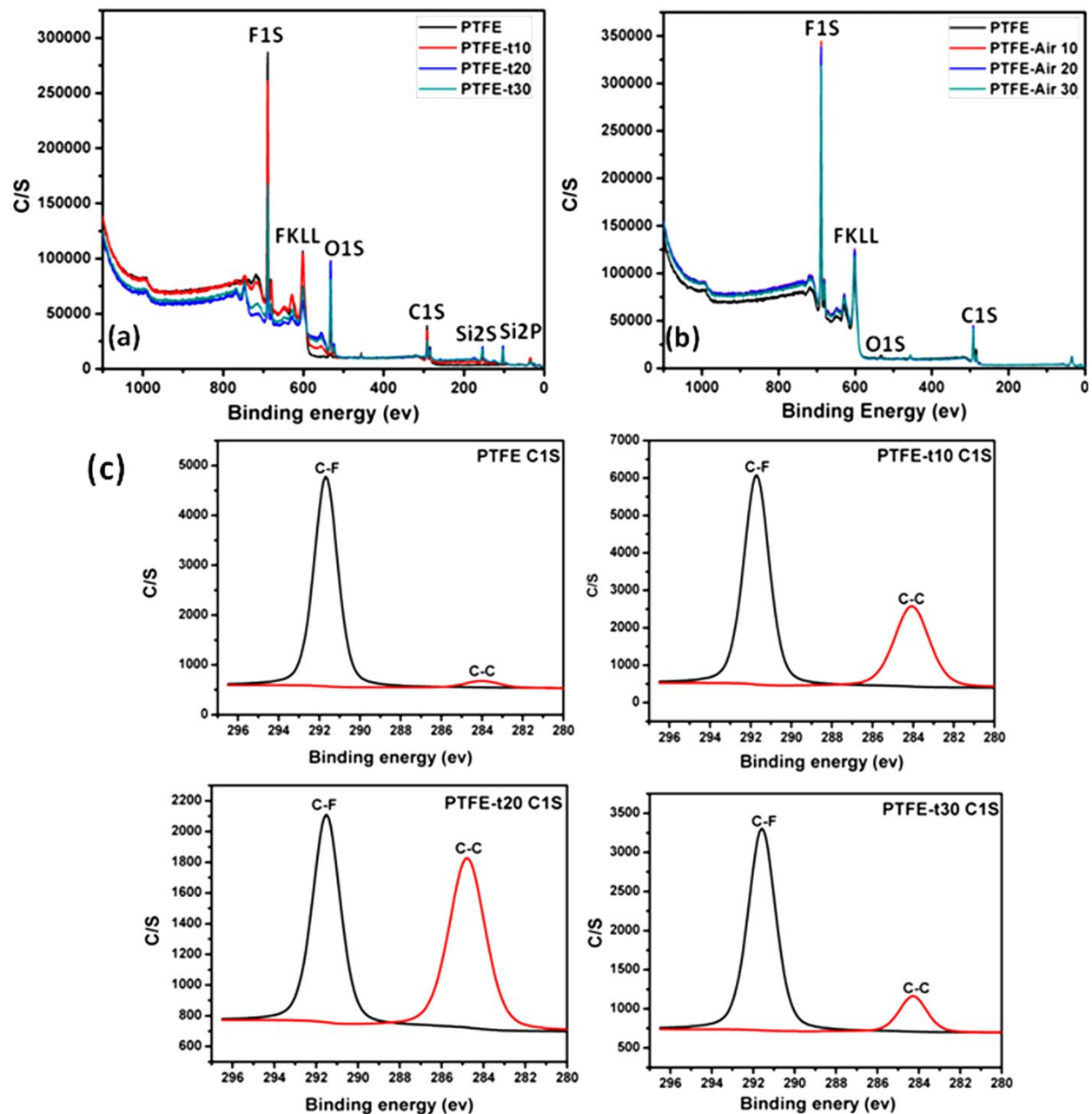
466 Figure 1: FTIR spectral analysis of the pristine PTFE, PTFE-t10, PTFE-t20 and PTFE-t30 surfaces

467 (a), Comparison of pristine PTFE, PTFE-Air 10, PTFE-Air 20 and PTFE-Air 30 surfaces (b),

468 Raman spectral analysis of the pristine PTFE, PTFE-t10, PTFE-t20 and PTFE-t30 surfaces in the

469 spectral range 180-1350 cm<sup>-1</sup> (the inset of the graph represents the magnified spectral region470 from 650-900 cm<sup>-1</sup>) (c), Raman spectral analysis of the pristine PTFE, PTFE-t10, PTFE-t20 and471 PTFE-t30 surfaces in the spectral range 2800-3500 cm<sup>-1</sup>.

472



473

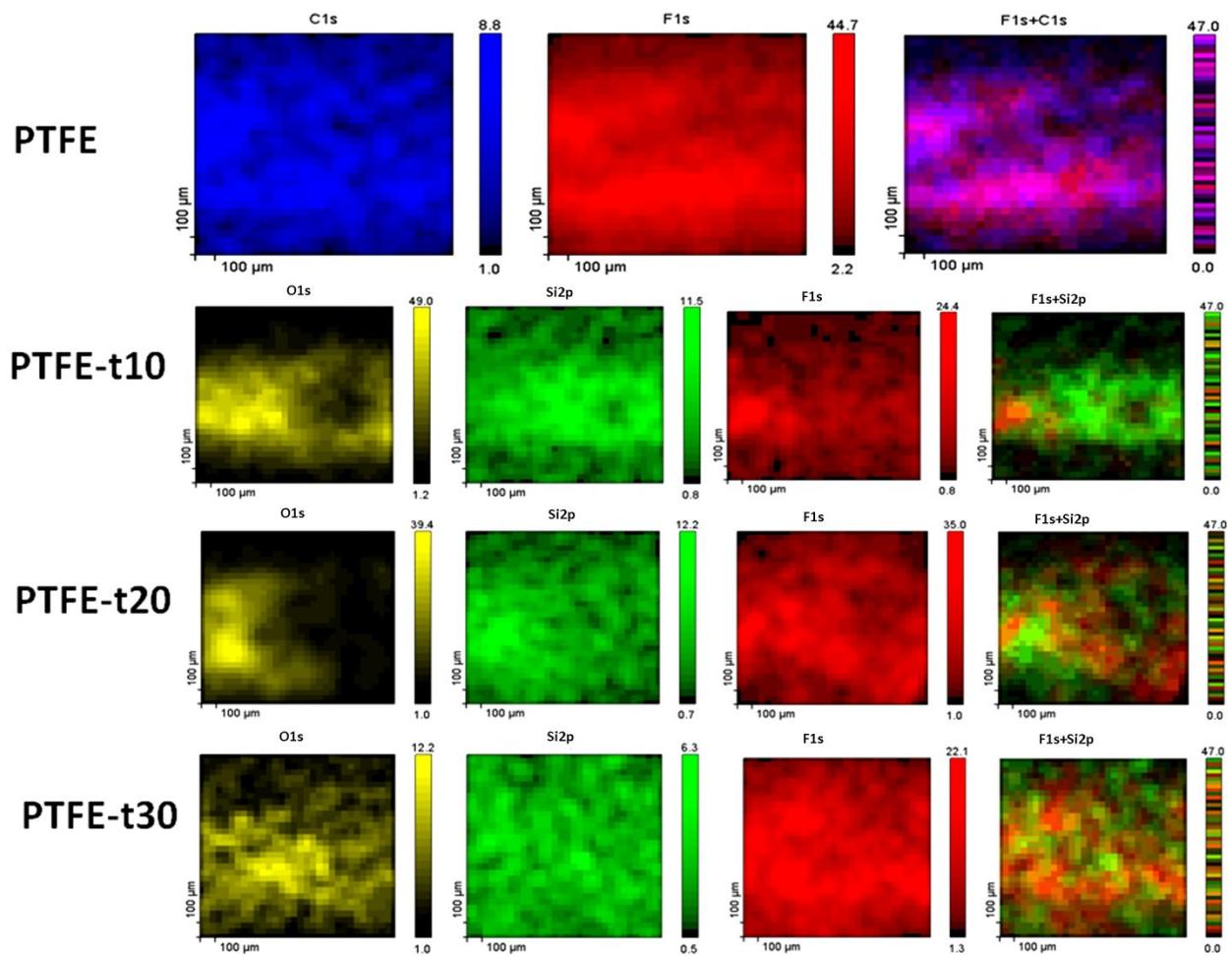
474 Figure 2: XPS comparison of the pristine PTFE,PTFE-t10,PTFE-t20 and PTFE-t30 surfaces (a),

475 Comparison of pristine PTFE and air plasma modified PTFE at different time periods (b), High

476 resolution C1S XPS spectrum of pristine PTFE,PTFE-t10,PTFE-t20 and PTFE-t30 surfaces (c).

477

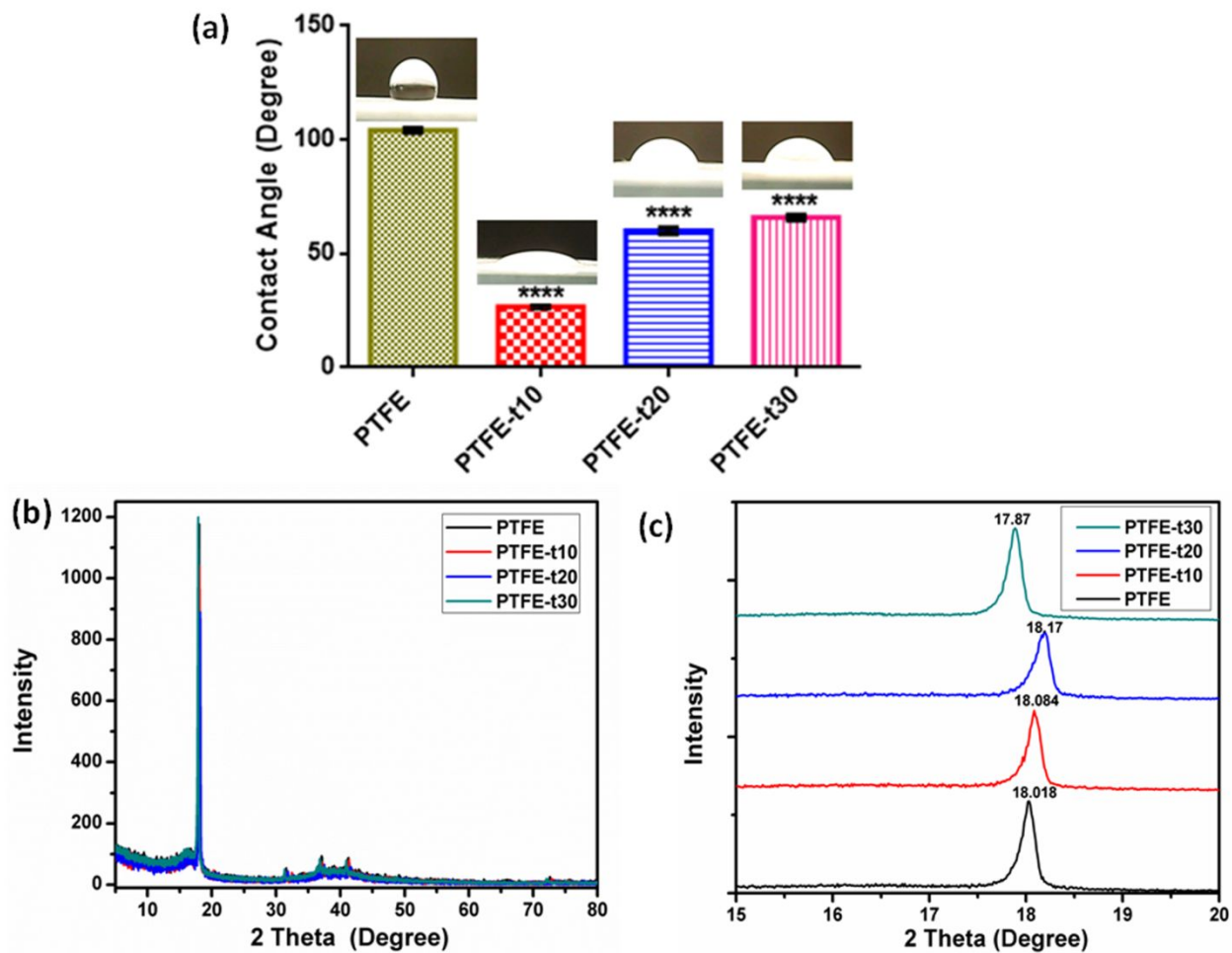




478

479 Figure 3: XPS chemical mapping images of the pristine PTFE, PTFE-t10, PTFE-t20 and PTFE-  
480 t30 surfaces.

481



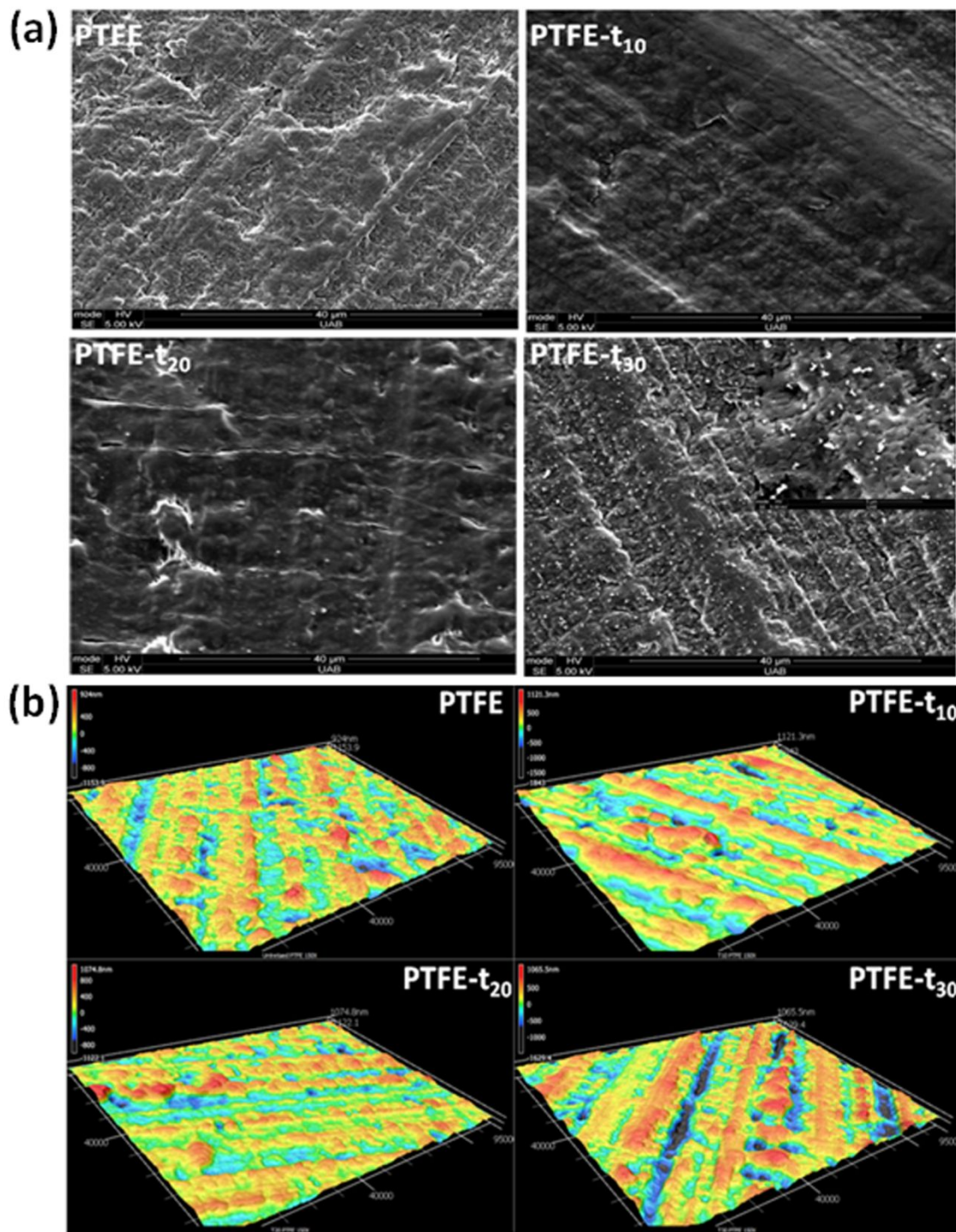
482

483 Figure 4: Contact angle measurements of pristine PTFE, PTFE-t10, PTFE-t20 and PTFE-t30  
 484 surfaces (a), X ray Diffraction experiments on pristine PTFE, PTFE-t10, PTFE-t20 and PTFE-t30  
 485 surfaces (b), Magnified X ray Diffraction spectra ( $2\theta$  ranging 15-20°) on pristine PTFE, PTFE-  
 486 t10, PTFE-t20 and PTFE-t30 surfaces (c).

487

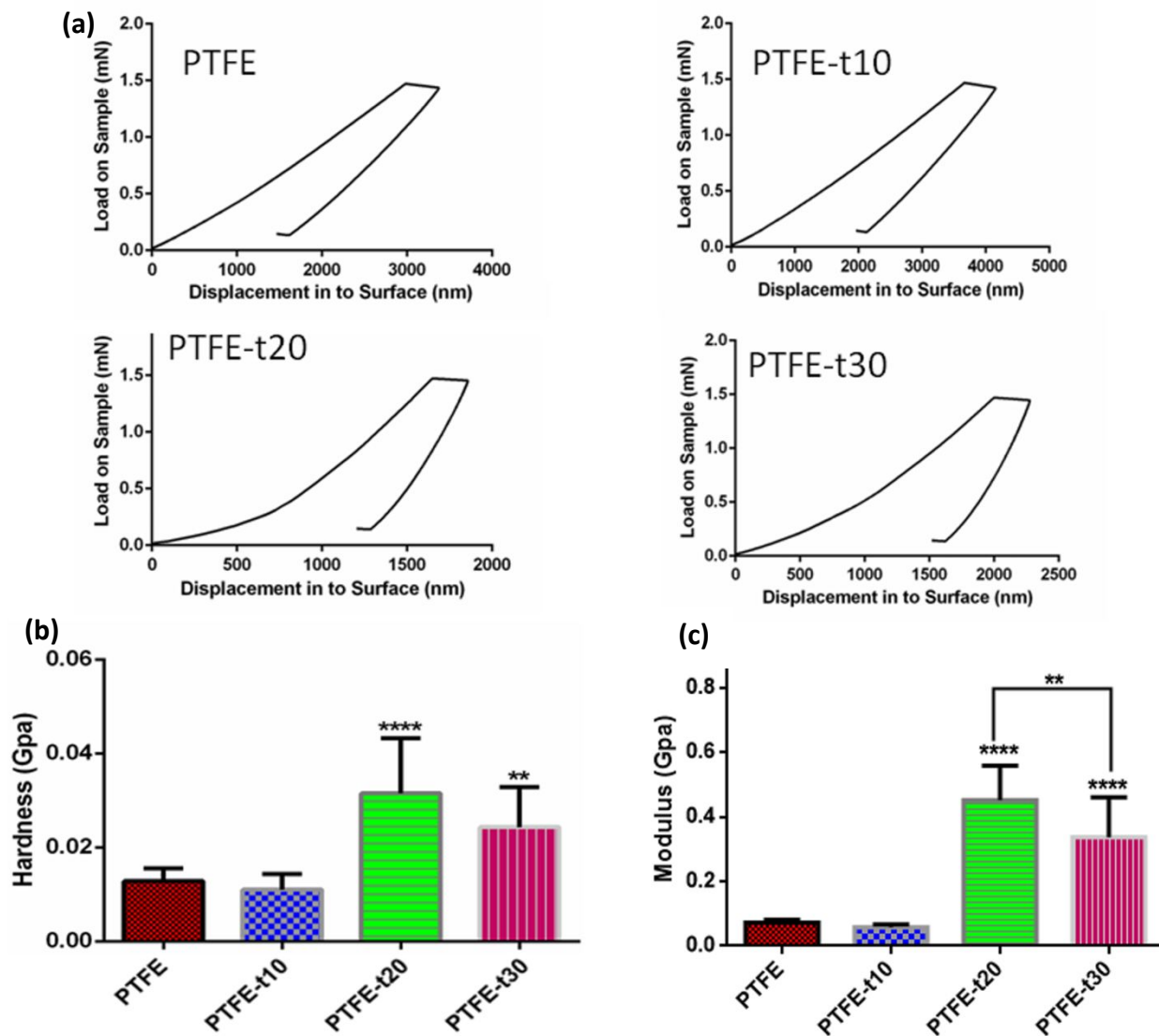
488

489



490

491 Figure 5: Scanning electron microscopy of pristine PTFE,PTFE-t10,PTFE-t20 and PTFE-t30  
492 surfaces (a), 3D laser scanning confocal microscopy images of the pristine PTFE,PTFE-  
493 t10,PTFE-t20 and PTFE-t30 surfaces (b).



494

495 Figure 6: Nanoindentation studies on pristine PTFE,PTFE-t10,PTFE-t20 and PTFE-t30 surfaces

496 (a), Hardness comparison on pristine PTFE,PTFE-t10,PTFE-t20 and PTFE-t30 surfaces (b)

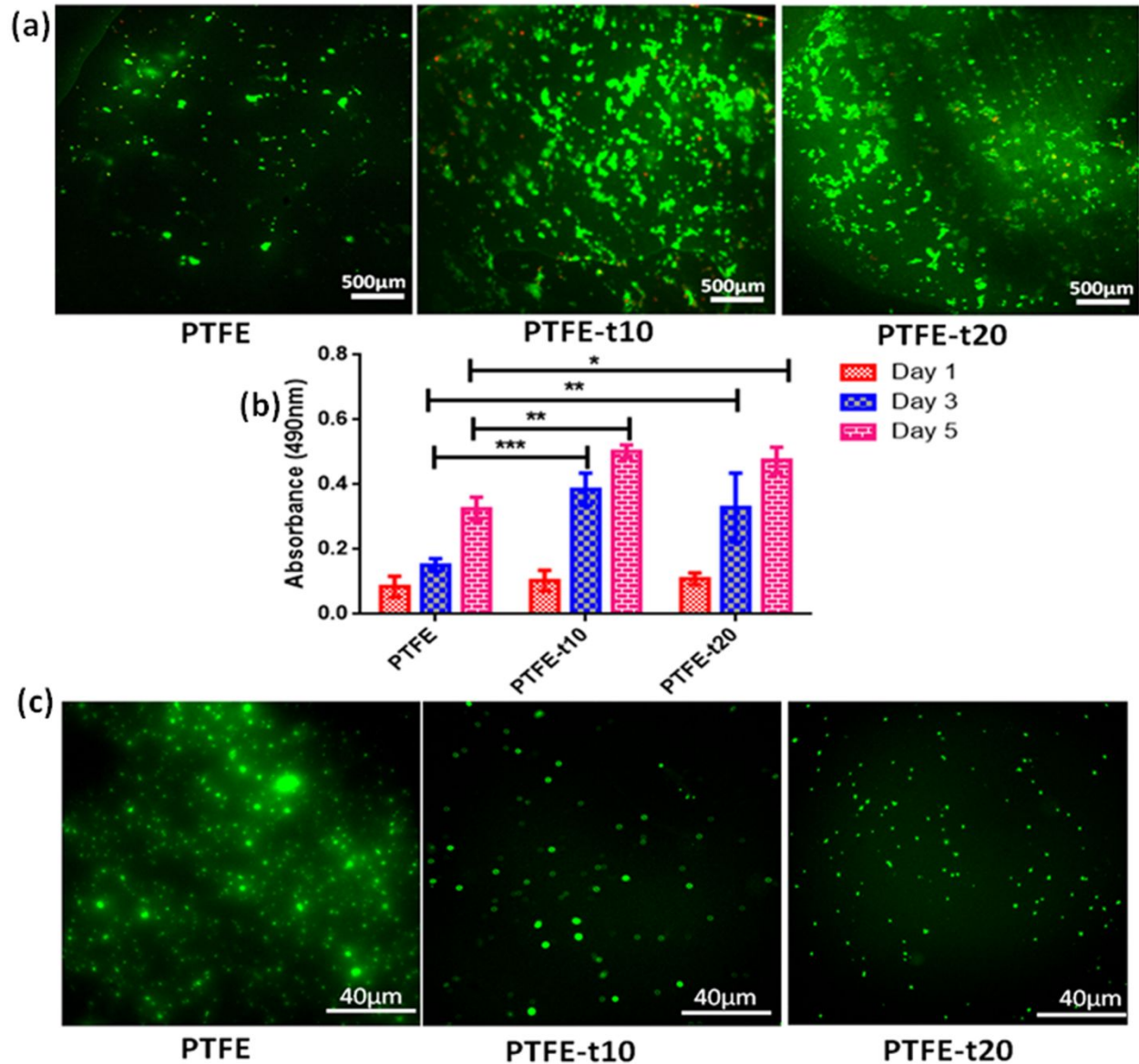
497 Elastic modulus comparison on pristine PTFE,PTFE-t10,PTFE-t20 and PTFE-t30 surfaces.

498

499

500



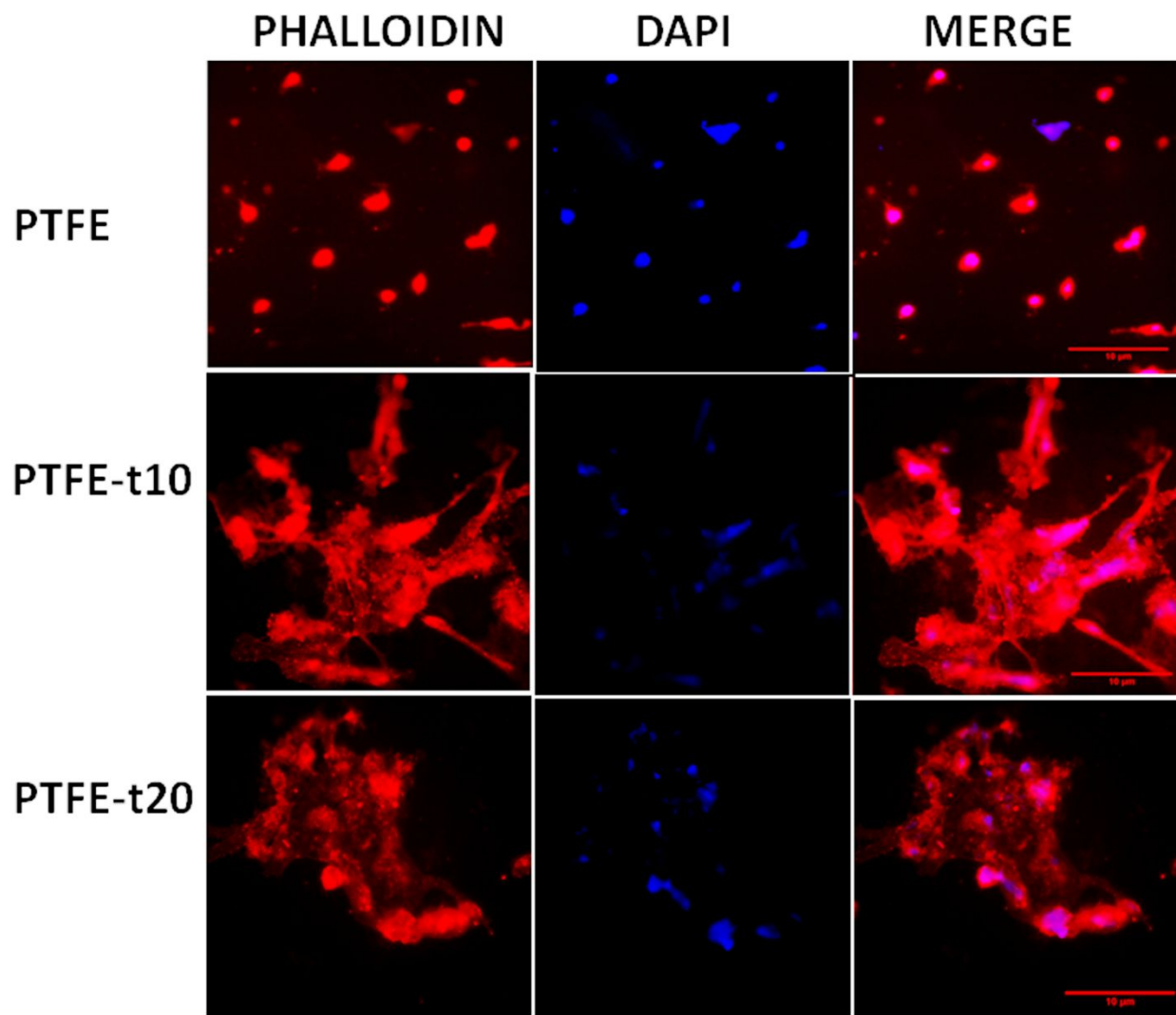


501

502 Figure 7: Live/dead assay on pristine PTFE, PTFE-t10 and PTFE-t20 surfaces after 3 days of  
 503 endothelial cell seeding (a), MTS assay on pristine PTFE, PTFE-t10 and PTFE-t20 surfaces after  
 504 1, 3 and 5 days of endothelial cell seeding (b) Platelet adhesion studies on pristine PTFE, PTFE-  
 505 t10 and PTFE-t20 surfaces (c).

506

507



508

509 Figure 8: Rhodamine Phalloidin cytoskeleton staining on pristine PTFE, PTFE-t10 and PTFE-t20  
510 surfaces after 3 days of endothelial cell seeding.

511

512

513

514

515

516

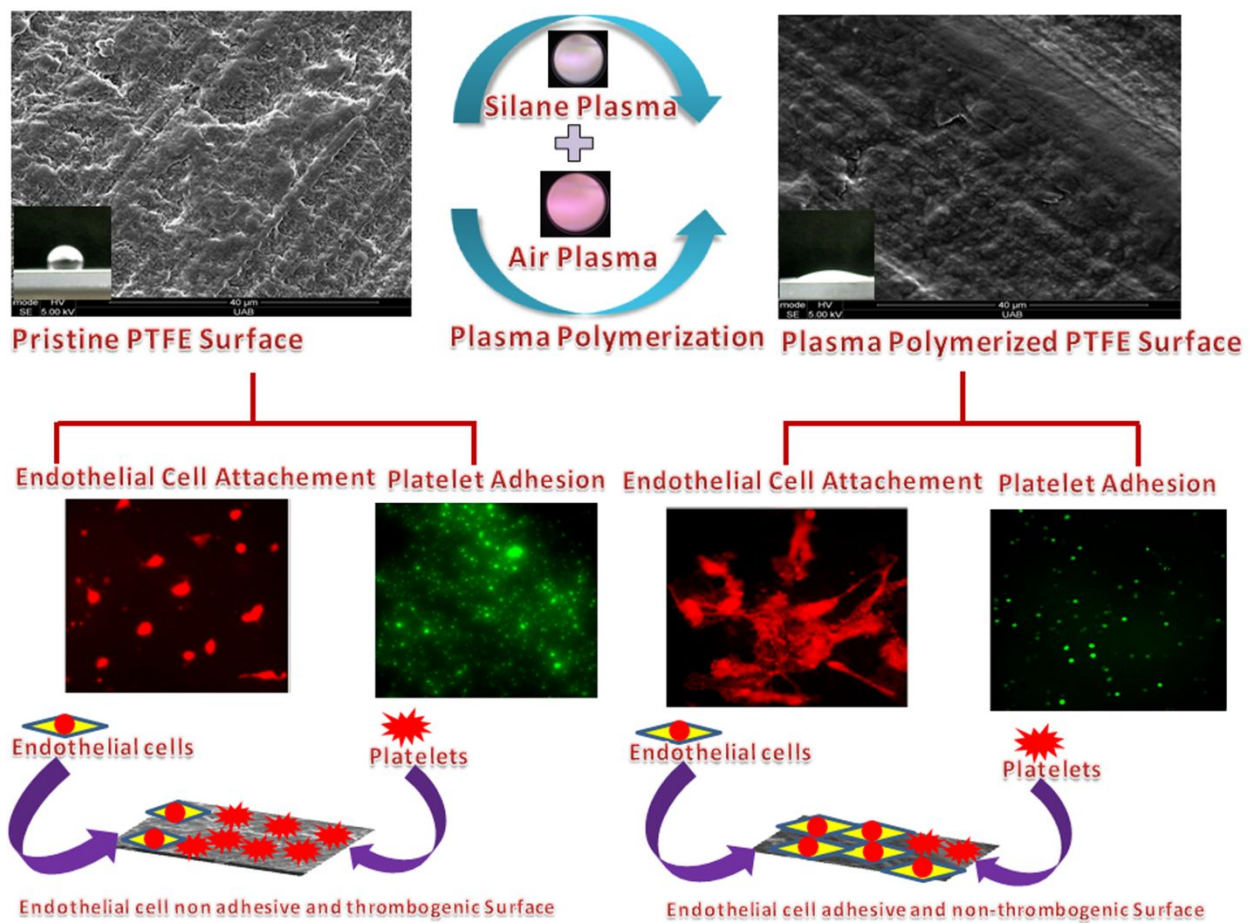
517

518

519

**Graphical Abstract/ TOC Graphics**

520



521